Journal of Power Sources 195 (2010) 1031–1037

Contents lists available at ScienceDirect

Journal of Power Sources

journal homepage: www.elsevier.com/locate/jpowsour

Modified polyol synthesis of PtRu/C for high metal loading and effect of post-treatment

Kug-Seung Lee, Hee-Young Park, Yong-Hun Cho, In-Su Park, Sung Jong Yoo, Yung-Eun Sung*

School of Chemical & Biological Engineering and Research Center for Energy Conversion & Storage, Seoul National University, Seoul 151-744, South Korea

ARTICLE INFO

Article history:
Received 6 April 2009
Received in revised form 25 June 2009
Accepted 4 August 2009
Available online 25 August 2009

Keywords:
Polyol reduction
Phase separation
Platinum–ruthenium catalyst
Methanol electro-oxidation

ABSTRACT

The polyol-reduction method is modified for both high metal loading and high dispersion of particles. The catalysts are post-treated with different atmospheres and temperatures. The post-treatment modifies the morphological and crystallographic structures of the catalysts which influence the methanol oxidation activities. The catalysts are characterized by using X-ray diffraction, transmission electron microscopy, and cyclic voltammetry. The post-treatment induces a change of surface areas and a phase separation of Pt and Ru that modify the surface structures along with the intrinsic and mass-specific activities of methanol oxidation. The activities modified by the post-treatment are investigated by using methanol oxidation at room temperature and at 60 °C. Comparison with single-cell performance is conducted, and the results are in accord with those for methanol oxidation at 60 °C. All synthesized catalysts exhibit higher single-cell performances than the commercial catalyst.

1. Introduction

Direct methanol fuel cells (DMFCs) have been considered ideal power sources for portable electronic devices. Much research on methanol electro-oxidation has been conducted to find optimal materials, surface structures, and synthetic methods. PtRu bimetallic materials are known to be most promising electrodes and the best Pt:Ru ratio has been reported to be 1:1.

Synthetic methods for PtRu alloy nanoparticles with appropriate surface structures and large surface areas have been investigated, e.g., impregnation, colloidal and microemulsion methods [1–6]. One of the most powerful methods is the polyol-reduction method using ethylene glycol (EG) as a solvent and a reducing agent along with controlling of the pH of the solvent with NaOH [5,7–9]. Glycolate acts as a stabilizer for the PtRu colloids and the size of the resulting colloids is controlled via the pH of the solution. The carbon-supported PtRu catalyst (PtRu/C) in the above publications showed an excellent dispersion of particles and greatly enhanced methanol oxidation activity.

In order to achieve a high dispersion of particles on the carbon support, the colloidal particles must exhibit strong repulsion forces against one another on their surfaces, which can be realized in the polyol method by controlling the pH of the solution with NaOH. As the pH of the solution increases, the size of the particles decreases and the particle dispersion on the carbon support can be enhanced. Metal loading on the carbon inevitably decreases due to the strong interparticle repulsion forces [10]. In a practical DMFC system, the metal loading should be high because of the low activity of the catalysts and the limited mass transport in a thick catalyst layer. Therefore, it is desirable to achieve a high metal loading on the carbon while the dispersion of the particles also remains high.

In this work, 60 wt.% PtRu/C catalysts are synthesized using a modified polyol-reduction method. The synthesized catalysts are post-treated at different temperatures and atmospheres. The surface structures and electrocatalytic activities of the catalysts change according to post-treatment conditions. The electrochemical characteristics and single-cell performance of the catalysts are compared with those of a commercial catalyst.

2. Experimental

2.1. Synthesis of PtRu/C

All aqueous solutions were prepared with deionized (DI) water, which was further purified with a Mili-Q system (Millipore water, 18.2 MΩ cm). The following chemicals were obtained from Aldrich: $H_2PtCl_6{\cdot}xH_2O$, $RuCl_3{\cdot}xH_2O$, ethylene glycol (99.8%). Sodium hydroxide beads (98%) were purchased from Samchun chemicals. All chemicals were of analytical grade and were used as-received.

The procedure for synthesizing PtRu/C was as follows: Pt ($H_2PtCl_6{\cdot}xH_2O$, 0.6 g) and Ru ($RuCl_3{\cdot}xH_2O$, 0.258 g) precursors were dissolved in 200 ml of EG solution containing 0.1 M NaOH. The solution was refluxed in a three-neck flask at 160 °C for 5 h in an argon

* Corresponding author. Tel.: +82 2 880 1889; fax: +82 2 888 1604.
E-mail address: ysung@snu.ac.kr (Y.-E. Sung).

0378-7753/$ – see front matter © 2009 Elsevier B.V. All rights reserved.
doi:10.1016/j.jpowsour.2009.08.051

atmosphere and then cooled naturally. Apart from synthesis of the PtRu colloid, 0.1 g of carbon black (Vulcan XC-72R) was dispersed in 600 ml of DI water through ultrasonic vibration. An adequate amount of PtRu colloid to make a mixture of 60 wt.% PtRu/C was added to the carbon-dispersed solution and mixed. After 30 min of vigorous stirring, 20 ml of 1 M H_2SO_4 were added to the solution and then the solution was heated at 70 °C for 1 h to achieve a high loading of PtRu colloid on the carbon support. Without this heating step, the maximum PtRu loading was 20 wt.% despite controlling the pH of the solution with various amounts of H_2SO_4. After natural cooling, the solution was filtered and evaporated. The obtained 60 wt.% PtRu/C catalyst was divided into three parts, and the three samples were post-treated in a tube furnace under three different conditions: (1) at room temperature in a 10% H_2/Ar atmosphere; (2) at 160 °C in a 10% H_2/Ar atmosphere; (3) at 160 °C in an air atmosphere for 1 h. The consequent catalysts are designated as H_2-RT, H_2-160d and Air-160d according to the post-treatment conditions of room temperature in a 10% H_2/Ar atmosphere, 160 °C in a 10% H_2/Ar atmosphere and 160 °C in an air atmosphere, respectively. The characteristics of all the catalysts were compared with those of a commercial catalyst (60 wt.% PtRu/C, E-TEK^{SM}).

2.2. Characterization

X-ray diffraction (XRD) analysis was performed using a Rigaku D/MAX 2500 instrument operated with a Cu K_α source (λ = 1.541 Å) at 40 kV and 200 mA. The samples were scanned from 20° to 80° (2θ) at a scan rate of 2° min^{-1}. Transmission electron microscopy (TEM) images were obtained with a JEOL 2010 transmission electron microscope operated at 200 kV. The samples were prepared by dispersing a small amount of powder in ethanol by means of ultrasonic treatment. Then, a drop of the dispersion was taken by a pipette and put on a carbon-coated copper grid and dried in air at 70 °C.

Cyclic voltammetry was performed in a conventional three-electrode electrochemical cell using a glassy carbon electrode (6 mm diameter) as a working electrode, Pt wire as a counter electrode, and a saturated calomel electrode (SCE) as a reference electrode [11,12]. Electrochemical measurements were all recorded and reported vs. a normal hydrogen electrode (NHE). The glassy carbon (GC) electrode was polished with 1, 0.3 and 0.05 μm-Al_2O_3 slurry and washed ultrasonically with DI water before use. The ink slurry was prepared by mixing carbon-supported nanoparticles, DI water, a 5 wt.% Nafion® solution (Aldrich Chem. Co) as a binding material and 2-propanol. 600 μl of Nafion® solution and 10 ml of 2-propanol per 0.1 g of electrocatalysts were mixed and then stirred until a homogeneous ink slurry was formed. A constant amount of ink slurry was dropped on the GC electrode with a micropipette, and the GC electrode was then dried in a vacuum oven. Electrochemical experiments were performed with an Autolab general purpose electrochemical system (Eco Chemie).

Electrochemical measurement was conducted in 0.5 M H_2SO_4 solution that was purged with nitrogen gas for 30 min prior to each test. Subsequently, three consecutive scans were performed in the potential range 0.05–0.8 V vs. NHE at a scan rate of 20 mV s^{-1}. CO stripping voltammetry was performed at potentials between 0.05 and 1.0 V vs. NHE at a scan rate of 20 mV s^{-1}. CO molecules were attached to catalysts at a potential of 0.1 V vs. NHE by bubbling a 0.5 M H_2SO_4 solution with 10% CO/He gas for 20 min and then the CO gas dissolved in the solution was removed by bubbling with Ar gas for 30 min. For measurement of the methanol oxidation reaction (MOR), a solution of 0.5 M H_2SO_4/1 M CH_3OH was purged with nitrogen gas prior to measurement. Cyclic voltammetry was conducted between 0.05 and 1.0 V vs. NHE at a scan rate of 20 mV s^{-1} at room temperature and 60 °C.

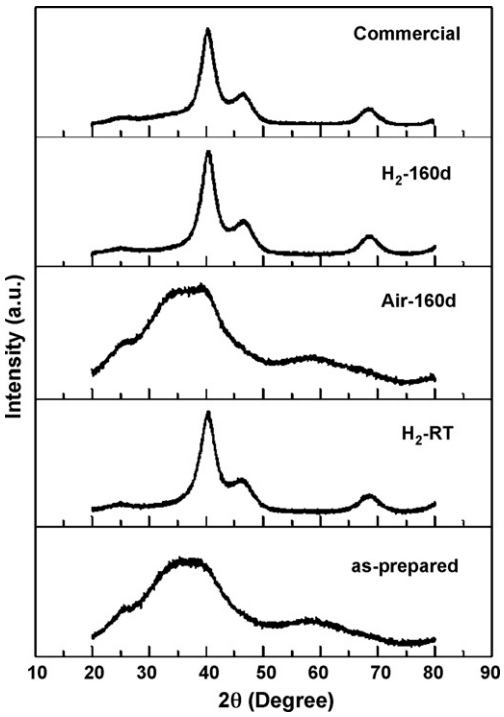

Fig. 1. XRD patterns of polyol-synthesized and commercial catalysts.

2.3. MEA fabrication and single-cell performance measurements

The catalysts tested in the present study were applied as anode catalysts and a commercial Pt black catalyst (Johnson Matthey) was applied as the cathode catalyst. The catalyst-coated membrane (CCM) was constructed by spraying the catalyst ink directly on to the polymer electrolyte membrane. Nafion 115 was used as the membrane, and the catalyst loading was 1.5 mg cm^{-2} on both sides of the membrane. Anode and cathode gas-diffusion layers were then placed on both sides of the CCM [13]. Polarization curves for each MEA were measured in individual 5 cm^2 cells. The MEA was placed between two gas-diffusion layers (GDLs), inserted into two graphite plates that contained a serpentine flow-field, and then assembled at a uniform torque. The single cell was then connected to a fuel cell test station (FCTS, WonATech Co., Ltd.) that consisted of a methanol pump, a mass flow controller, and electrical heaters to control the temperature. A 1 M methanol solution and air were fed respectively into the anode and cathode sides of the single cell to measure the performance of the MEA. The feed rate of the 1 M methanol solution and air were 1 and 90 ml min^{-1} for the anode and cathode, respectively. The temperature of the single cell was maintained at 60 °C [14].

3. Results and discussion

3.1. Structural characterizations

In order to investigate the crystallographic structures of the catalysts, XRD measurements were performed and the results are presented in Fig. 1. The as-prepared catalyst shows superposed peaks of RuO_2 diffractions at 35° (1 0 1) and 58° (2 2 0), and Pt diffractions at 39.7° (1 1 1) and 67.8° (2 2 0). The clear observation of RuO_2 may come from the heating step for the deposition of particles on carbon. The hot acidic environment of the solution may attack OH-groups on the particle surface and oxidize Ru during the heating step. Without the heating step, PtRu colloidal particles were partially deposited on carbon (to produce 20 wt.% PtRu/C)

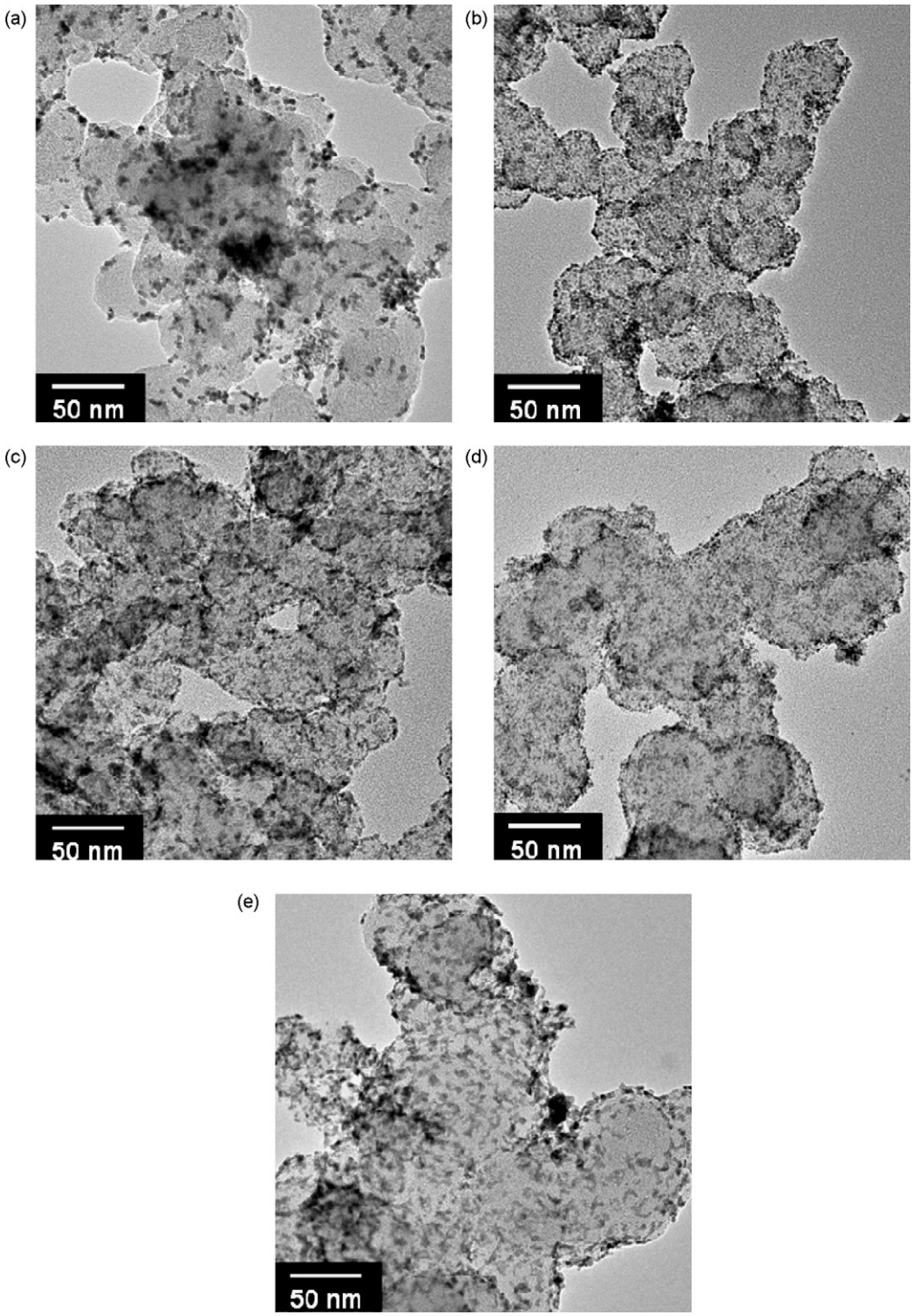

Fig. 2. TEM images of (a) commercial, (b) as-prepared, (c) H_2-RT, (d) Air-160d and (e) H_2-160d catalysts.

and the remainder fell through the filter paper during the filtering step. This 20 wt.% PtRu/C gave a PtRu alloy diffraction pattern without RuO_2 diffraction (data not shown). The commercial, H_2-RT, and H_2-160d catalysts represent typical PtRu alloy diffraction peaks at 40.3, 46.5 and 68.4° for Pt (1 1 1), (2 0 0), and (2 2 0), respectively [15]. The Pt diffraction peaks shift to higher 2θ degree (e.g., pure Pt (1 1 1) diffraction peak is found at 39.7°), and this indicates that the Ru element is incorporated into the Pt FCC lattice to form a PtRu alloy. The absence of RuO_2 diffraction in the H_2-RT catalyst indicates that most of the RuO_2 in the as-prepared catalyst is reduced by the H_2 flow at room temperature. Particle sizes calculated using the Scherrer equation and the Pt (2 2 0) peak are 3.4, 2.9 and 3.1 nm for commercial, H_2-RT and H_2-160d catalysts, respectively. The Air-160d catalyst exhibits similar diffractions to the as-prepared catalyst but the Pt diffraction peaks at 39.7 and 67.8° are slightly sharp compared with those of the as-prepared catalyst. This means that the RuO_2 and Pt phase are separated further during the post-treatment.

TEM images of the catalysts were obtained in order to observe morphological structures, and are shown in Fig. 2. The particles in the commercial catalyst are severely agglomerated on the carbon support with a particle size of 2–5 nm. By contrast, the catalysts

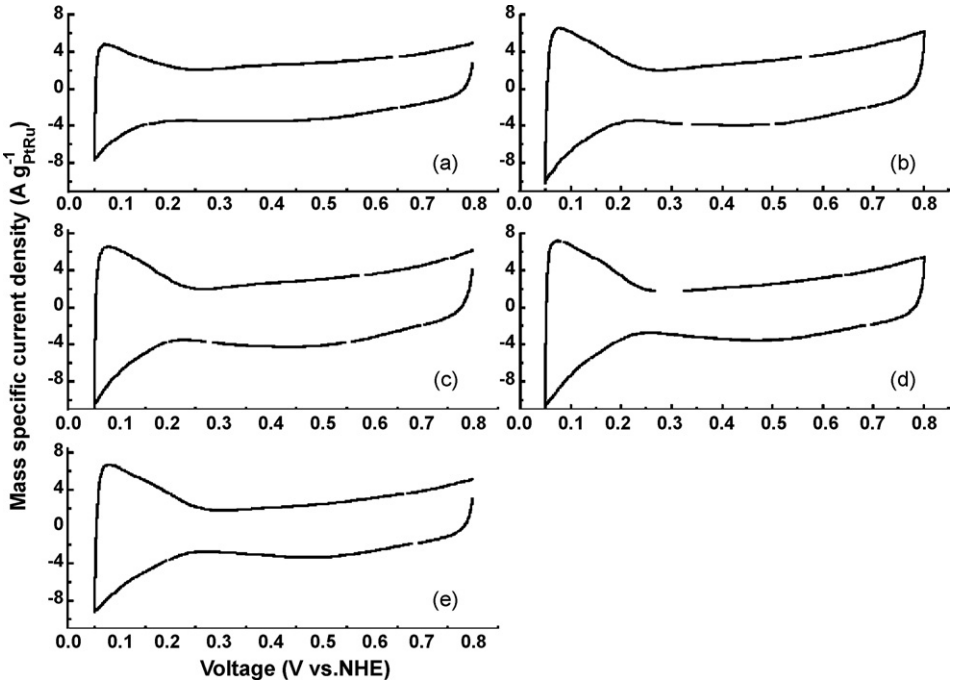

Fig. 3. Cyclic voltammograms of (a) commercial, (b) as-prepared, (c) H_2-RT, (d) Air-160d and (e) H_2-160d catalysts in 0.5 M H_2SO_4.

synthesized by the modified polyol method show a good dispersion of particles on the carbon support although the dispersion degree is different from one to another. The particles of the H_2-RT catalyst are slightly agglomerated compared with those of the as-prepared catalyst, and the particles of the H_2-160d catalyst are agglomerated further. This indicates that the H_2 flow modifies the morphological structures of the catalysts to reduce surface areas during the post-treatment. The Air-160d catalyst exhibits similar particle dispersion to the as-prepared catalyst due to the oxygen in air during the post-treatment [16]. Mean particle diameters in TEM images are 2.6, 2.9, 3.3 and 2.6 nm for the as-prepared, H_2-RT, Air-160d and H_2-160d catalysts, respectively. This indicates that post-treatment changes the size of the particles as well as their dispersion on carbon. Post-treatment in a reductive atmosphere (10% H_2/Ar) induces agglomeration and growth of particles while that in an oxidative atmosphere (air) maintains the morphological structures of the particles.

3.2. Electrochemical characterization

The surface characteristics of nanoparticles are crucial since electrocatalytic reactions are sensitive to surface structures. Cyclic voltammograms obtained in 0.5 M H_2SO_4 at room temperature are given in Fig. 3. The currents are normalized by the PtRu mass in the catalysts. The PtRu/C catalysts show the typical profiles of PtRu alloy particles in the hydrogen and oxygen adsorption/desorption regions. On the other hand, somewhat different features are found in the voltammograms of the commercial and polyol-synthesized catalysts. In the hydrogen adsorption/desorption region (0.05–0.3 V), the commercial catalyst (Fig. 3a) shows a complete suppression of hydrogen adsorption/desorption on the Pt surface, which corresponds to the result of Gasteiger et al. [17]. A shoulder peak at 0.18 V is found in the polyol-synthesized catalysts and this peak becomes prominent in the catalysts that were post-treated at higher temperatures. In addition, the positions of the oxygen desorption peaks at 0.3–0.6 V are also found to be different from one another. The oxygen desorption peaks are located at 0.36, 0.43, 0.45 and 0.48 V for the commercial, H_2-RT, Air-160d and H_2-160d catalysts, respectively. The shoulder peak in the hydrogen adsorption/desorption region and the positive shift in oxygen desorption peak can be attributed to less Ru-rich surfaces and/or phase separation of Pt and Ru [17–19]. Phase separation during post-treatment can occur and the surface states of the catalysts differ depending on the temperature and atmosphere. In the PtRu alloy system, Pt has a lower surface energy in vacuum and can be segregated on the surface at reasonable temperatures. The segregation can be significantly modified in the presence of an oxygen adsorbate since the strong binding between Ru and O on the surface surpasses the higher surface energy of Ru [20]. McNicol and Short [21] studied the surface enrichment phenomena of PtRu catalysts at 300–500 °C in H_2 and an air atmosphere. Cyclic voltammetric studies of the catalyst surface revealed that heating in H_2 produced a surface resembling pure Pt while samples heated in air showed typical Ru-rich profiles. Hwang et al. [22] reported similar results using X-ray absorption spectroscopy analysis. In the present experiment, the degree of surface composition change may be lower than that found in previous studies because the temperature of the post-treatment is lower. Among the catalysts in the present study, the H_2-160d exhibits the greatest change in surface composition while the H_2-RT undergoes the least change. Thus the change in composition depends on the temperature of the post-treatment. The Air-160d does not show a Ru-rich surface, although it was post-treated in air atmosphere. This may be attributed to the RuO_2 already formed in the as-prepared catalyst, as demonstrated by XRD analysis. That is, oxygen in the air atmosphere at the temperature does not course a Ru-rich surface to form and further separates the already formed Pt and RuO_2 phases on the surface.

CO stripping analysis was performed to investigate the CO tolerance and the electrochemical active surface area (ESA) of the catalysts. The results are given in Fig. 4. CO stripping and methanol oxidation reaction (MOR) data of the as-prepared catalyst are almost the same as those of the Air-160d or in-between the Air-160d and H_2-RT catalysts, so they are not included in Figs. 4 and 5 for clarity. The peak potentials of the catalysts not very different from each other, namely, 0.52, 0.52, 0.54 and 0.54 V for the commercial, H_2-RT, Air-160d and H_2-160d catalysts, respectively. This

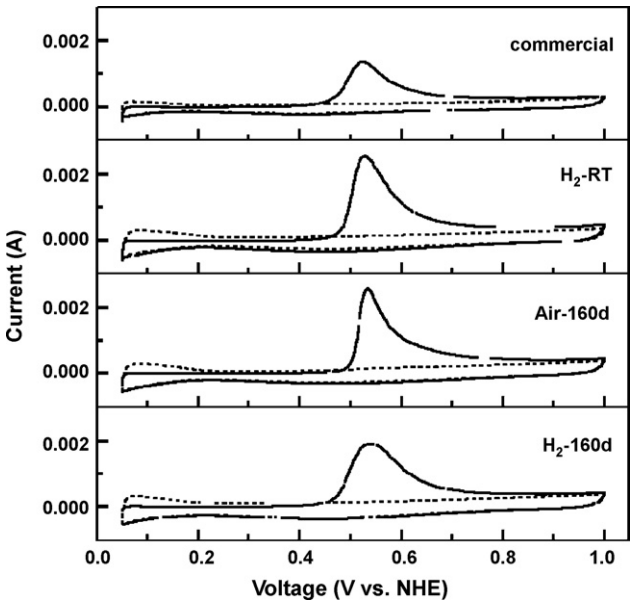

Fig. 4. CO stripping voltammograms of catalysts in 0.5 M H_2SO_4.

indicates that the commercial and H_2-RT catalysts are more tolerant to CO poisoning than the Air-160d and H_2-160d catalysts. Gasteiger et al. [23] reported CO stripping analysis on various compositions of PtRu catalysts. The lowest peak potential was found for a Pt:Ru surface composition of nearly 1:1, and the peak potential of a catalyst with a surface composition of 2:1 was observed at a more positive potential by 0.03 V. Similar results were reported by Bock et al. [24]. Although the peak potentials in the present experiment are not the same as those of the above studies, the difference in peak potentials (0.02 V) of the prepared catalysts may indicate that the difference in the surface compositions of the catalysts are within the results of previous studies. The ESA of the catalysts was calculated using CO stripping charges and yielded values of 50.7, 72.8, 75.8 and 65.4 $m^2\,g_{PtRu}^{-1}$ for the commercial, H_2-RT, Air-160d and H_2-160d catalysts, respectively. The polyol-synthesized catalysts have higher ESAs than the commercial one. Among the polyol-synthesized catalysts, the highest ESA is found for the Air-160d and the lowest ESA for H_2-160d. These findings are in accord with the TEM analysis, where particles in the Air-160d are found to be well-dispersed and similar to the as-prepared catalyst whereas particles in the H_2-160d are agglomerated.

3.3. Methanol oxidation

MOR was carried out at room temperature and at 60 °C to compare the oxidation activities of the catalysts under the two different conditions. The oxidation current was normalized by the CO stripping area (for surface-specific current density) and by the mass of PtRu (for mass-specific current density), as shown in Fig. 5. Electrocatalytic activities of catalysts are affected by the active surface area, amount of loaded catalyst, and the intrinsic activity [25]. If the amount of loaded catalyst is fixed, the activity can be influenced by the two other factors. The surface-specific current density represents the intrinsic activity while the mass-specific current density represents both the active surface area and the intrinsic activity. The surface-specific current density of the catalysts at room temperature (Fig. 5a) shows that the catalysts post-treated at higher temperatures are more active than the commercial and H_2-RT catalysts (0.44, 0.35, 0.29 and 0.24 A cm^{-2} for H_2-160d Air-160d, H_2-RT and the commercial catalyst at 0.5 V, respectively). By contrast, however, the surface-specific current density obtained at

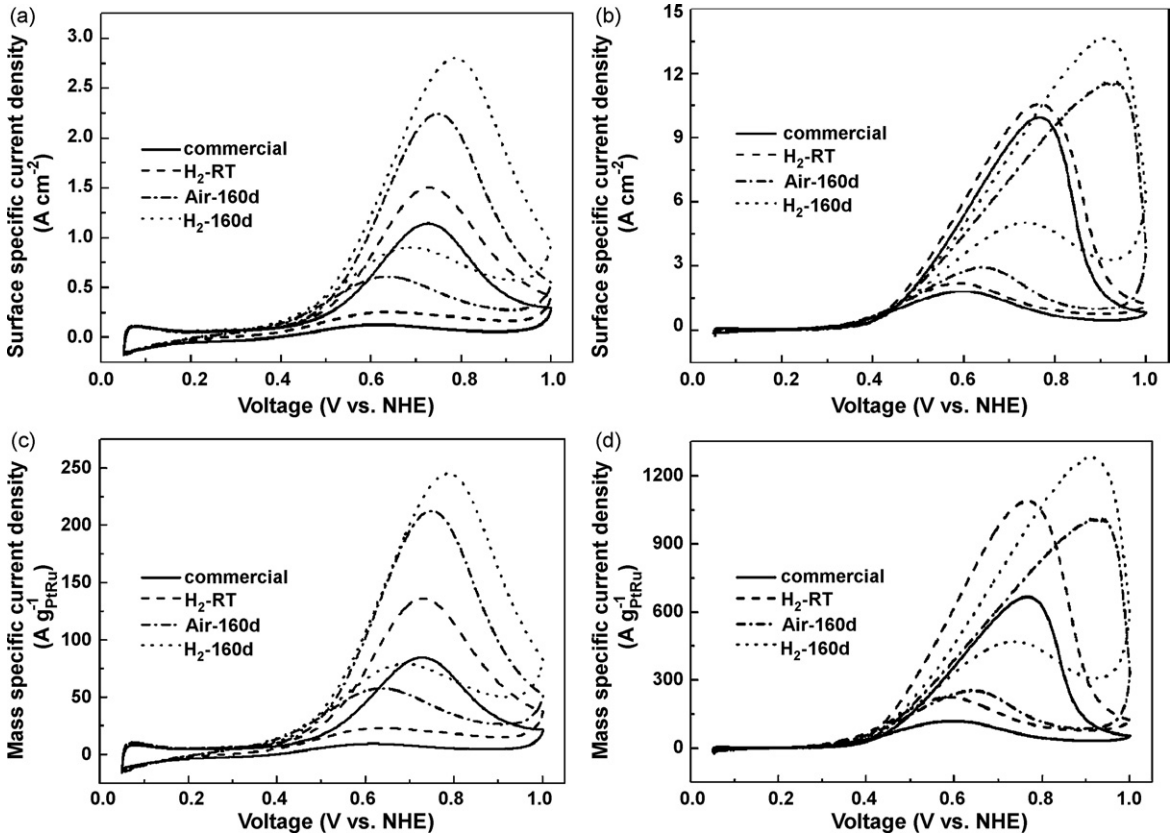

Fig. 5. Cyclic voltammetric analysis for methanol oxidation reaction in 0.5 M H_2SO_4/1 M CH_3OH at room temperature (a and c) and at 60 °C (b and d).

60 °C (Fig. 5b) reveals that the catalysts post-treated at higher temperatures are less active (2.7, 2.4, 2.3 and 2.1 A cm^{-2} for H_2-RT, the commercial, H_2-160d and Air-160d catalyst at 0.5 V, respectively), indicating that the order of intrinsic activity for the catalysts is changed by the temperatures of MOR. A shift in optimum composition with temperature on the PtRu thin film electrode was reported by Gasteiger et al. [26], who observed a shift in the Ru content for the optimum surface from 10% at room temperature to 30% at 60 °C. The shift in the optimum composition was attributed to a shift in the rate-determining step from methanol adsorption/dehydrogenation at the low temperature to the surface reaction between the dehydrogenated intermediate and surface oxygen at the high temperature. Bock et al. [24] calculated the theoretical percentage of catalyst utilization as a function of the Pt:Ru ratio, assuming that an assembly of three neighboring Pt and one Ru site are involved in the oxidation of a methanol molecule due to the suitable methanol adsorption. The optimum composition in the calculation was 30% Ru in the unsupported PtRu catalyst, which corresponded to the experimental results. In the present investigation, the post-treated catalysts exhibit a phase separation between Pt and Ru and may form a more favourable surface composition for methanol adsorption at room temperature. At a high temperature (60 °C), the role of Ru on the surface (removing the intermediate species) becomes more important, as suggested in the above report [26], and the commercial and H_2-RT catalysts show higher surface-specific activity.

Mass-specific activities at room temperature display the same trends (38, 33, 26 and 18 A g^{-1}_{PtRu} for the H_2-160d, Air-160d, H_2-RT and commercial catalysts at 0.5 V, respectively) as those of the surface-specific activities at room temperature. This means that ESA does not significantly affect the mass-specific activity at room temperature (although the effect must be noted). Mass-specific activities, however, at 60 °C show different trends (272, 206, 181 and 150 A g^{-1}_{PtRu} for the H_2-RT, H_2-160d, Air-160d and commercial catalysts at 0.5 V, respectively) from those of the surface-specific activities at 60 °C, which indicates that the effect of ESA is higher at 60 °C than at room temperature. For example, the commercial catalyst exhibits the highest surface-specific activity at 60 °C next to the H_2-RT, but the lowest mass-specific activity at the same temperature, due to the lowest ESA. The H_2-RT exhibits the highest activities for both surface-specific and mass-specific current densities at 60 °C. The highest activity of the H_2-RT catalyst may be attributed to the mild condition of the post-treatment so that the phase separation and the agglomeration of particles are both weak.

3.4. Single-cell performance

The single-cell performances were compared and are shown in Fig. 6. The result shows that the DMFC with the H_2-RT as anode catalyst has the highest cell voltage under the same discharging current density (0.088, 0.068, 0.046 and 0.032 A cm^{-2} at 0.4 V for the H_2-RT, H_2-160d, Air-160d and commercial catalysts, respectively) and the highest maximum power density (0.062, 0.054, 0.049 and 0.042 W cm^{-2} for the H_2-RT, H_2-160d, Air-160d and commercial catalysts, respectively), whereas the DMFC with the commercial catalyst has the lowest cell voltage and the lowest power density. The trend of increasing single-cell performance is the same as that of mass-specific activity for MOR at 60 °C, confirming that the comparison of the mass-specific activity for MOR at 60 °C accurately represents single-cell performances. The performance using the as-prepared sample as an anode catalyst is slightly higher than that of Air-160d and lies between those of Air-160d and H_2-160d, similar to the result of MOR (data not shown). Therefore, the single-cell performances prove that the catalysts synthesized by the modified polyol method are more active than the commercial catalyst, and

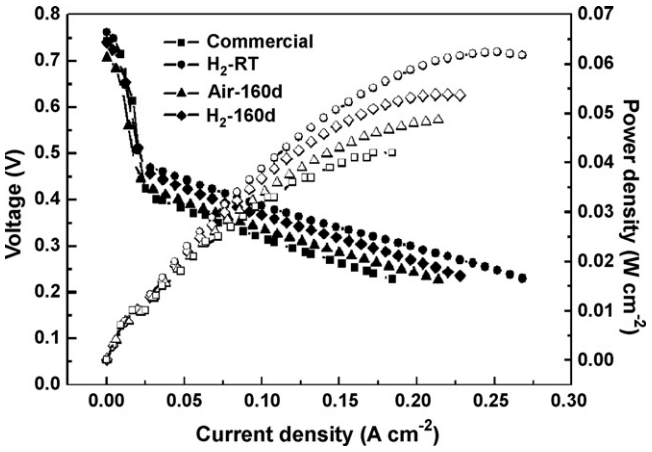

Fig. 6. Polarization and power density curves of single cells using prepared samples as anode catalysts at 60 °C.

that the mild condition of the post-treatment (H_2-RT) leads to the most active surface structure for methanol oxidation.

4. Conclusions

The polyol-reduction method has been modified to produce PtRu/C catalysts with high metal loading. The prepared catalysts are post-treated under three different conditions. The surface of the as-prepared catalyst is modified under the three different conditions of post-treatment. The modified surface structures may be attributed to the phase separation of Pt and Ru in the post-treatment atmosphere. The catalysts synthesized by the modified polyol method display different activity trends in MOR at room temperature and 60 °C, which can be attributed to a shift in the rate-determining step from methanol adsorption/dehydrogenation at the low temperature to a surface reaction between the dehydrogenated intermediate and surface oxygen at the high temperature. Among the synthesized catalysts, the H_2-RT catalyst exhibits the highest intrinsic activity and thereby is the most efficient surface structure for MOR due to the mild conditions of the post-treatment. The H_2-160d and Air-160d catalysts have lower intrinsic activities due to the phase separation. The synthesized catalysts exhibit higher mass-specific activities compared with the commercial catalyst due to the higher ESA. The single-cell performance is found to be in accordance with the MOR at 60 °C.

Acknowledgements

This work was supported by the Ministry of Commerce, Industry and Energy, the KOSEF through the Research Center for Energy Conversion & Storage and the Korea Research Foundation (Grant # KRF-2006-005-J04601).

References

[1] K.-Y. Chan, J. Ding, J. Ren, S. Cheng, K.Y. Tsang, J. Mater. Chem. 14 (2004) 505.
[2] H. Bönnemann, R.M. Richards, Eur. J. Inorg. Chem. 10 (2001) 2455.
[3] A. Roucoux, J. Schulz, H. Patin, Chem. Rev. 102 (2002) 3757.
[4] Z. Liu, J.Y. Lee, M. Han, W. Chen, L.M. Gan, J. Mater. Chem. 12 (2002) 2453.
[5] C. Bock, C. Paquet, M. Couillard, G.A. Botton, B.R. MacDougall, J. Am. Chem. Soc. 126 (2004) 8028.
[6] X. Zhang, K.-Y. Chan, Chem. Mater. 15 (2003) 451.
[7] J. Guo, G. Sun, S. Sun, S. Yan, W. Yang, J. Qi, Y. Yan, Q. Xin, J. Power Sources 168 (2007) 299.
[8] J. Guo, G. Sun, Z. Wu, S. Sun, S. Yan, L. Cao, Y. Yan, D. Su, Q. Xin, J. Power Sources 172 (2007) 666.
[9] P. Kim, J.B. Joo, W. Kim, J. Kim, I.K. Song, J. Yi, J. Power Sources 160 (2006) 987.
[10] H.-S. Oh, J.-G. Oh, Y.-G. Hong, H. Kim, Electrochim. Acta 52 (2007) 7278.

[11] T.H. Hyeon, S.G. Han, Y.-E. Sung, K.-W. Park, Y.-W. Kim, Angew. Chem. Int. Ed. 43 (2003) 4252.
[12] I.-S. Park, B. Choi, D.-S. Jung, Y.-E. Sung, Electrochim. Acta 52 (2006) 1683.
[13] Y.-H. Cho, B. Choi, Y.-H. Cho, H.-S. Park, Y.-E. Sung, Electrochem. Commun. 9 (2007) 378.
[14] Y.-H. Cho, H.-S. Park, Y.-H. Cho, I.-S. Park, Y.-E. Sung, Electrochim. Acta 53 (2008) 5909.
[15] I.-S. Park, K.-W. Park, J.-H. Choi, C.R. Park, Y.-E. Sung, Carbon 45 (2007) 28.
[16] T.R. Ralph, M.P. Hogarth, Platinum Met. Rev. 46 (2002) 117.
[17] H.A. Gasteiger, N. Marković, P.N. Ross, E.J. Cairns, J. Phys. Chem. 97 (1993) 12020.
[18] T. Vidaković, M. Christov, K. Sundmacher, K.S. Nagabhushana, W. Fei, S. Kinge, H. Bönnemann, Electrochim. Acta 52 (2007) 2277.
[19] D.C. Papageorgopoulos, M.P. de Heer, M. Keijzer, J.A.Z. Pieterse, F.A. de Bruijin, J. Electrochem. Soc. 151 (2004) A763.
[20] B.C. Han, A. Van der Ven, G. Ceder, B.-J. Hwang, Phys. Rev. B 72 (2005) 205459.
[21] B.D. McNicol, R.T. Short, J. Electroanal. Chem. 81 (1977) 249.
[22] B.-J. Hwang, L.S. Sarma, G.-R. Wang, C.-H. Chen, D.-G. Liu, H.-S. Sheu, J.-F. Lee, Chem. Eur. J. 13 (2007) 6255.
[23] H.A. Gasteiger, N. Marković, P.N. Ross, E.J. Cairns, J. Phys. Chem. 98 (1994) 617.
[24] C. Bock, B. MacDougall, Y. LePage, J. Electrochem. Soc. 151 (2004) A1269.
[25] K.-S. Lee, I.-S. Park, Y.-H. Cho, D.-S. Jung, N. Jung, H.-Y. Park, Y.-E. Sung, J. Catal. 258 (2008) 143.
[26] H.A. Gasteiger, N. Marković, P.N. Ross, E.J. Cairns, J. Electrochem. Soc. 141 (1994) 1795.